Low filling ratio acoustic space filling curve metamaterials for jet engine inlets

LOW FILLING RATIO ACOUSTIC SPACE FILLING CURVE METAMATERIALS FOR JET ENGINE INLETS

JN Glover PhD Student, Department of Aeronautical and Automotive Engineering, Loughborough University, UK
DJ O'Boy Senior Lecturer in Structural Dynamics, Department of Aeronautical and Automotive Engineering, Loughborough University, UK

1 INTRODUCTION

As pressure grows for aircraft noise control, from organisations like the Advisory Council for Aircraft Research and Innovation in Europe (ACARE) there is an increased need for innovation in Aeroacoustic attenuation. The nature of noise means that a targeted approach to attenuation is far more effective in achieving overall observable noise reductions. Therefore, this project focuses on the dominant noise source, the engine, which accounts for approximately 68% at approach and at take-off approximately 98% of the total aircraft noise [1] (percentage of total logarithmic dB output). Any solution needs to cope with extreme operating conditions and low frequency noise not commonly controlled by traditional methods, due to the long wavelengths involved. This paper introduces innovative metamaterial acoustic liners as solutions for the jet engine inlet and builds on the work by Glover and O'Boy 2020 [2].

Metamaterials demonstrate a huge resource for acoustic control whether passively in coiling-up, Helmholtz resonator like or membrane structured, as reviewed in the paper by Assouar et al [3]. Or actively with piezoelectric, mechanical or electric and magnetic biasing as discussed in "A Review of Tunable Acoustic Metamaterials" [4]. For this project, the metamaterials studied are Space Filling Curves (SFC) defined by their sub-wavelength structural, curled cross section. They are classed as a passive absorber acoustic liner. The SFC provides an elongated coiled propagation path able to attenuate much lower frequencies then an undivided cavity of the same dimensions. They are not governed by traditional bulk modulus and density characteristics. SFC offer subwavelength low frequency attenuation with the potential to provide a lightweight, thin, high performance acoustic liner [3]. The present paper contains a comparison of some of the most promising low filling ratio metamaterial designs which utilise Space Filling Curves. It evaluates the liners in terms of the fundamental theory of the design and a discussion of the reflection and absorption characteristics. The design of the original inspiration for this method are provided, then the paper discusses computer simulation and experimental testing to compare the different designs based on impedance tube measurements. Conclusions are also made as to the future application for aeroacoustics with particular focus on the engine inlet.

2 ACOUSTIC LINERS

Typical acoustic liners for a commercial jet engine use the principle of a Helmholtz Resonator (HR) where a mass of air oscillates on a spring of air trapped in a volume. HR implementations are cheap passive devices, are relatively lightweight and effective for one dominant frequency and most importantly, need a large depth to attenuate low frequencies. The issue of low frequency attenuation is due to the mass law. The effect is essentially, the lower the desired attenuation frequency the larger the liner depth needs to be [5] (and for the purposes of this paper the frequency range of interest is 200-2000Hz). By targeting one dominant frequency, any other

frequencies are not substantially affected, and the same weight penalty remains. Hence, the choice of critical frequency and the potential for multiple frequency targeting is paramount.

The liners are proposed to control the dominant frequencies of jet engines, typically below 1000Hz, with the lowest at approximately 630Hz by Khardi [6]. Moreover, the industrial trend towards ultra-high bypass engines means there is a potential increase in bypass ratio from 8 to 15 [7]. Since ultra-high bypass fans result in an increase in weight and potential drag it is predicted that there will be a subsequent reduction in the thickness of the outer casing, meaning that any soundproofing contained within needs to become thinner [7]. Therefore, in this paper the depth of the liners is tightly controlled bellow 50mm, the lower end of typical current liner depth. A successful metamaterial acoustic liner would show a reduced weight and thickness compared to a traditional HR liner, i.e. a low filling ratio design (the filling ratio is the proportion of wall volume to open air volume). By utilising the sub-wavelength attenuation and high reflective nature of SFC a significant sound reduction can be achieved with a relatively low weight liner. In addition, a 2020 paper by Glover and O'Boy concludes that low filling ratio SFCs generate a higher mean absorption coefficient when tested in head on flow conditions [2].

2.1 Helmholtz resonator

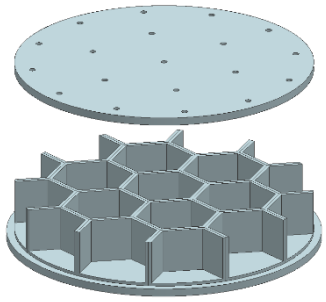

Figure 2-1 Helmholtz Resonator 610Hz

Traditional Helmholtz Resonators (HR) are used to control steady, simple harmonic sound at a narrow frequency range. The main advantages of this resonator is its simplicity, although careful tuning is required for effective noise attenuation [8]. The HR works as an acoustic stopband filter with the action of the volume of air in the cavity emulating a mass spring system [8]. However, this causes an undesirable back pressure which has a detrimental effect on the efficiency and performance of the engine. The limited narrow band can be improved with a range of tuned HRs, but this has a proportional increase in back pressure [5]. If frequency bands could be filtered out through an alternative method such as multi-resonant scattering, there would be a far smaller effect on engine efficiency which could be a designed in characteristics of metamaterial liners.

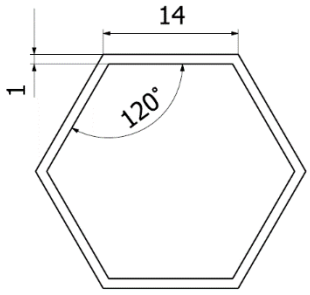

Figure 2-2 Helmholtz Resonator 610Hz unit cell

For the purposes of comparison in this paper a baseline acoustic liner was designed using a hexagonal 610Hz tuned HR (Figure 2-1 and Figure 2-2), see formula in [7]. This design was also used in the 2020 paper [2]. This was chosen to compromise between industry standard design, the working frequency range of the experimental impedance tube and available 3D printing capabilities allowing rapid prototyping and experimental verification of the trends. The hexagonal HR liner was a benchmark of success criteria for the SFC liners. Thus, a good liner would show a better absorption coefficient at a wider frequency range and ideally at a lower weight. The additional characteristics of a typical sandwich configuration was also applied to the SFCs for the following three reasons: 1) The two microphone impedance set up doesn't allow for the grazing configuration and the tube was designed to record head-on resonance for sandwich liners. 2) A sandwich configuration is the current standard for soundproofing thus can be considered commercial. 3) The additional resonant conditions are predicted to improve absorption coefficients for the SFC samples.

2.2 Space Filling Curves

Space-filling curve (SFC) metamaterials are designed with a sub-wavelength curled wave path creating a mazelike pattern (Figure 2-3). SFC were developed from a purely mathematical problem where a line passes through every cell element of a grid, so that every cell is visited exactly once. They have been proposed in acoustics for a decade or so due to their potential ultra-thin, low

frequency, broadband attenuation overcoming the drawbacks of traditional HRs. In this paper, three designs are investigated, termed horn, meander and spider. For the purposes of this project the investigated SFC designs are divided into two categories; curl-up (horn and meander) where there is a single path through a unit and maze-like (spider) where there are multiple propagation directions within the unit. To understand the advantages of metamaterials as a noise control method there needs to be an appreciation of the physical attenuation mechanisms.

Figure 2-3 Spider SFC liner model

The primary physical mechanism of noise reduction in both types is an extended pathlength compared to unit depth, which enables subwavelength attenuation. Different designs can offer multiple propagation paths, directions, and scattering. For curl-up SFC's, (Figure 2-6) Wang et al [9] have proposed an equivalent model which applies HR, and quarter wavelength (QWR) tube theory to, a ranging transfer matrix that defines the SFC peak frequency. The transfer matrix establishes a relationship between the acoustic pressure and volume velocities in 2 defined regions.

Equation 2-1 Relationship between the acoustic pressure and volume velocities at the neck of the tube and the end of the cavity [9]

$$\begin{bmatrix} p_{in\_I} \\ U_{in\_I} \end{bmatrix} = \begin{bmatrix} cosk{l'}_n & -j\frac{\rho c}{S_I} sink{l'}_n \\ j\frac{S_I}{\rho c} sink{l'}_n & cosk{l'}_n \end{bmatrix} \begin{bmatrix} cosk{l'}_n & -j\frac{\rho c}{S_I} sink{l'}_n \\ j\frac{S_I}{\rho c} sink{l'}_n & cosk{l'}_n \end{bmatrix} \begin{bmatrix} p_{out\_II} \\ U_{out\_II} \end{bmatrix}$$

Equation 2-1 shows the two regions the first is a straight region which is the straightened coiling path (denoted I) equated to a resonator neck and the second is a cavity region which would be designated voids (denoted II). When region 1 tends to zero the HR theory alone applies and when region 2 tends to zero the quarter wavelength theory alone applies. The curl-up SFC studied in this project (horn, meander and zig-zag from a previously published paper) all build on classical theory. The resonant frequency for a the same volume of HR unit can be reduced by making use of curling channels to reduce the space required: QWR uses Equation 2-2, HR uses Equation 2-3 and Fabry-Perot resonance (FP) using Equation 2-4. The use of voids, framing, right angle bends and many other flow path features causes the SFC resonance to deviate from the basic theory which is why models such as the equivalent model transfer matrix are used [9]. Although this approximation works well for curled up designs it is less accurate for the maze like SFC's such as the spider.

Equation 2-2 QWR resonant frequency

$$f_{res} = \frac{c(2n-1)}{4L}$$

Equation 2-3 HR resonant frequency

$$f_{res} = \frac{c}{2\pi}\sqrt{\frac{S}{LV}}$$

Equation 2-4 FP resonant frequency

$$f_l^{FP} = \frac{lc_0}{2L_{eff}}$$

The maze-like designs are better understood using Mie resonant theory as they offer multiple propagation directions and a high reflective index. Mie resonance is commonly defined in light rather than sound, but it still applies when the size of the scattering sphere is comparable to the wavelength. Mie-resonance particles have a high refractive index relative to background medium. They are initiated in this case due to the ultraslow relative propagation through the flow path compared to the in space dimensions (Figure 2-4) [10]. These liners often benefit from multiple resonances instigated at low frequency due to the high contrast of sound speed with the isotropic resonant frequency shown in Equation 2-5. The proposed spider maze-like metamaterial is described as being an ultra-slow medium demonstrating the high contrast in wave speed needed to observe Mie resonance [11].

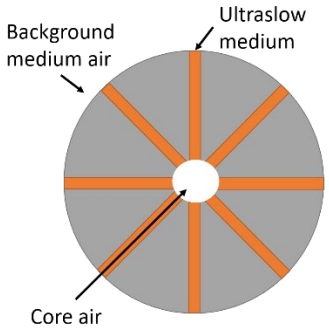

Figure 2-4 Ultra slow fluid medium representation of spider liner

Equation 2-5 Isotropic Mie resonant frequency[12]

$$f = \frac{c}{\pi n_r}\sqrt{\frac{2\eta}{R_i(R-R_i)'}}$$

It was predicted that the low filling ratio (<20%) characteristic of these three designs could result in an overall reduction in weight whilst, maintaining or improving noise attenuation in a broadband low frequency range.

2.2.1 Horn

The first acoustic liner design investigated was proposed by Ghaffarivardavagh et al. [13] named ''Horn-like space-coiling''. This design was an advancement of the zig-zag configuration based on Liang and Li [14] adding a gradual change in channel width allowing for impedance matching. The sample presented by Ghaffarivardavagh et al. was tested computationally with the Transfer Matrix Method based on computer modelling, using the finite element analysis software COMSOL. Then it was experimentally validated as a large rectangular sample with a 40cm measurement region much larger than the sample in Figure 2-6 which is 95mm in diameter.

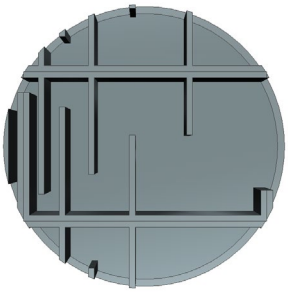

Figure 2-5 Horn SFC liner model

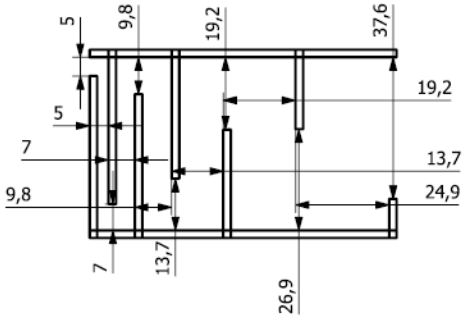

Figure 2-6 Horn liner unit

This design termed horn was chosen as it was capable of phase-amplitude modulation beyond conventional space-coiling structures, with a potential for sound focusing and acoustic beam splitting. The sample seen in Figure 2-6 and unit sizing (Figure 2-7) was inspired by Ghaffarivardavagh et al. [13]. A custom 1kHz design with 1% transmission coefficient. The test liner was tessellated (Figure 2-6) to cover the whole 95mm diameter space available in the test rig (See Figure 3-1). The filling ratio of horn was 9.4%, therefore is considered very low and the sample was the lightest of the 3 SFCs. It is the only liner lighter than the HR baseline (Table 4-1). The Ghaffarivardavagh et al. [13] data was presented only as transmission coefficient whereas the 2 microphone impedance method only establishes reflection and absorption coefficient. For comparison, the peak transmission 1000Hz was taken as the peak absorption frequency although as discussed in section 2.2.3 this may not be an accurate representation.

2.2.2 Meander

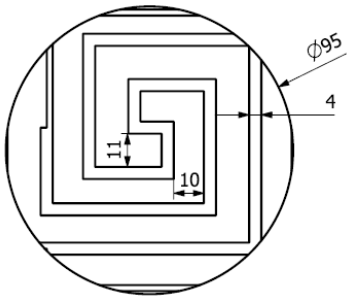

Figure 2-7 Meander liner unit

The “Coiling-Up Space Metasurfaces” was developed by Chen et al. is the second design under investigation in this paper [15]. This design is an acoustic metasurface with a perforated top plate and co-planer spiral tubes in coiling channels. It was tested using simulation in COMSOL and validated with an impedance tube method. Unlike the horn or spider liners or any of the phase 1 samples (see Glover and O’Boy [2]) this was the only SFC design optimised with a perforated plate. This was a key factor in its inclusion in the study as a perforated plate is the standard for traditional liner constructions. Additionally, in high flow speed and long run time regions such as a jet engine inlet, foreign object debris is a substantial concern, thus the use of perforated plates has been the established prevention method.

The design shown in Figure 2-8 was developed based on the work by Chen et al. [15]. The channels act as nesting dampeners producing dual band resonance (in this case 256Hz and 350Hz). The thickness of the metasurface is smaller than 1/50 of the resonant frequency wavelength and set in the reproduced model as 20mm. This design is chosen as it has the lowest predicted resonant frequency and a low filling ratio of 14%. The performance of the design is particularly interesting because the predicted values are so close to the lower limit of the working frequency range therefore open to experimental error.

2.2.3 Spider

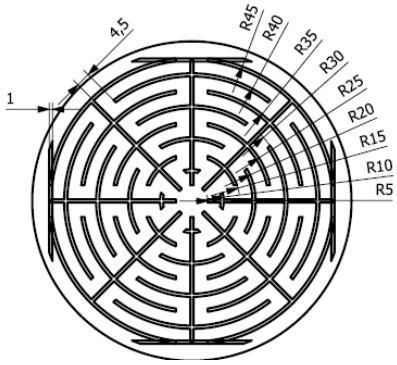

Figure 2-8 Spider liner unit

The “Spider web-structured labyrinthine acoustic metamaterials” was developed by Krushynska et al. is the final design under investigation [11]. This design configuration consists of a square external frame and a circular maze like path divided into eight independent circular-shaped channels connected at the centre. As a result of the need for consistency between the designs, the sample is circular and unframed (Figure 2-10). However, the advantages of framing will be studied in future work. Krushynska et al. tested the design using simulation in COMSOL only and demonstrated consistent low transmission for a frequency range 0-2000Hz. Unlike the horn or meander designs, the spider is classified as a mazelike SFC meaning there are multiple propagation routes rather than a singular flow direction. This design is also very difficult to predict through a numerical theory due to the presence of Mie scattering which is why the origin paper’s use of simulation is vital in predicting the acoustic performance.

The design shown in Figure 2-10 was inspired by garden spider *Araneus diadematus*. It was chosen due to its low filling ratio of 10% which is much smaller than that of the maze-like SFC studied in phase 1: 17% for hexagonal and 35% for labyrinthine [2]. In addition, Krushynska et al. concluded the spider SFC is highly tuneable with activation or elimination of subwavelength band gaps and negative group-velocity modes can be refined by increasing/decreasing the edge cavity dimensions. Like the horn work this design is presented via transmission rather than absorption thus the peak values may not consistently align. Absorption coefficient has two different formulas based on whether transmission is possible within the experimental setup (Equation 2-7 and Equation 2-8). Generally, absorption and reflection coefficients are mirror plots, but the transmission may not follow the same trend. As a result, the accuracy of this design recreation, particularly in terms of full range low transmission, will not be known fully until the four microphone impedance test stage which is not part of this paper.

Equation 2-6 Absorption coefficient for anechoic termination

$$\alpha = 1 - |R_a|^2 - |T_a|^2$$

Equation 2-7 Absorption coefficient for rigid termination

$$\alpha = 1 - |R_h|^2$$

3 IMPEDANCE TUBE RIG

3.1 Impedance tube theory

A two microphone Impedance tube (Figure 3-1) was designed and built to accurately measure sound reflection and absorption coefficients according to ISO10534-2 [16]. The basic principle of the tube is that a plane wave is generated by a sound source and measurements of acoustic pressure are taken at fixed locations depending on the number of microphones. The reflection or absorption through the sample generates a standing wave that can be measured by the microphones. A white noise source is used with no external flow applied. Calculations are carried out using a complex transfer function to determine the normal incidence absorption and impedance ratios of the acoustic material (Equation 3-1, Equation 3-2). The usable frequency range depends on the width of the tube and the spacing between the microphones (Figure 3-2) [16]. In this case the diameter of 100mm and length 500mm give a working range of 200-2000Hz. The origin papers are not all tested in the same standardised method or flow conditions therefore this paper experimental work can be uniquely compared.

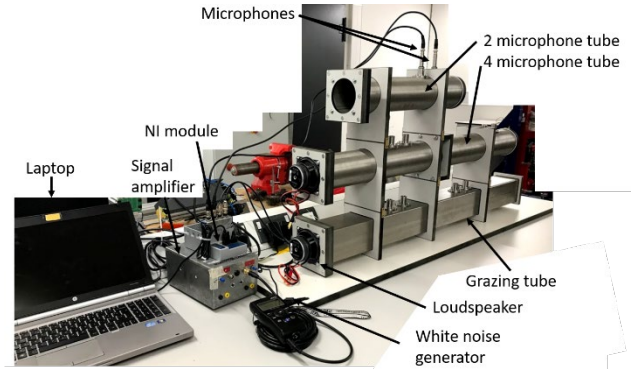

Figure 3-1 Photograph of experimental rig

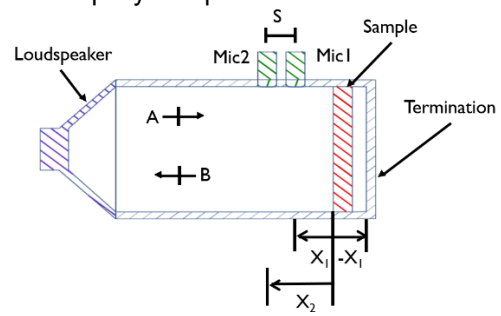

Figure 3-2- Two microphone impedance tube

Equation 3-1- Transfer Matrix Two Microphone Impedance Tube

$$\begin{bmatrix} p \\ v \end{bmatrix}_{x=0} = \begin{bmatrix} T_{11} & T_{12} \\ T_{21} & T_{22} \end{bmatrix} \begin{bmatrix} p \\ v \end{bmatrix}_{x=d}$$

4 EXPERIMENTAL ANALYSIS OF LINERS

4.1 Methodology

The experimental analysis determined the reflection and absorption coefficients of each liner by frequency and as a mean value. The data was then compared between the liners and the simulation results in the comparison papers. The liner samples were designed such that each core liner has a diameter of 95mm and a rigid backplate of 2.5mm. The core height is 15 mm for the horn SFC is based on the core height for the 610 Hz resonant HR baseline. As the meander and spider design stated their core height it was maintained in this case at 17 mm and 20mm. An additional variable of three designed top plates of thickness 2.5 mm and no top plate options were investigated. Each liner was tested with no top plate, the HRTP (Figure 4-1) and a many-hole top

plate. The meander used MTP (Figure 4-3) rather than MHTP (Figure 4-2) to match the perforated plate used in the origin paper experimental work. All components were printed using a Connex 260 and utilised a ‘’Vero White’’ plastic. The experimental analysis of all four liners followed the ISO10534-2 [16] protocol for a two microphone impedance tube. The weights can be found in Table 4-1.

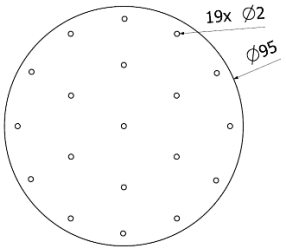

Figure 4-1 Helmholtz resonator top plate

Helmholtz Resonator Top Plate (HRTP). This perforated top sheet is designed specifically for the Helmholtz resonator.

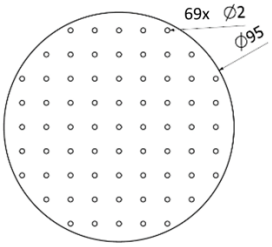

Figure 4-2 Multiple hole top plate

Multiple Hole Top Plate (MHTP). This perforated top sheet was designed to have the same orifice diameter as the HRTP but 69 holes.

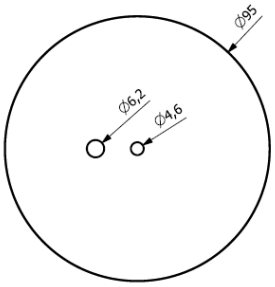

Figure 4-3 Meander top plate

Meander Top Plate (MTP). This perforated top sheet was designed based on the top plate proposed by Chen et al.[15]

Table 4-1 Acoustic liner and top plate weights

LINERS	WEIGHT (g)	TOP PLATES	WEIGHT (g)
Helmholtz Resonator	50	**Helmholtz Resonator**	21
Meander	60	**Many hole**	18
Horn	47	**Meander TP**	21
Spider	59		

4.2 Results

The absorption coefficient relationship to frequency is presented in Figure 4-4. There are common trends between all liners: the use of a top-plate has a significant increase on the overall absorption coefficient; the non top-plate configuration absorption values are consistent for all liners and there is no strong indication of the effect of the designed flow path without a top plate. An interesting deviation from the expected is the horn with MHTP which, unlike the other two SFCs and liner theory does not show an increase in peak frequency when more perforations are introduced. The theoretical peak increase as predicted by the work of Bies and Handen [17]. Conversely with MHTP the horn has a dual peak at 790 and 1590Hz compared to the HRTP 1430Hz. This change is assigned to an increase in the peak frequency associated with the resonant HR mechanism of the liner and the 790Hz peak aligns with an analytical study of Fabry-Perot resonance peak (Equation 2-4). For all designs, Figure 4-4 does not show peak frequencies that align closely with the origin paper. This is because there is a distinct difference between the sub-wavelength attenuation, transmission properties and resonance attenuation. This difference will be captured by the progression work of the project summarising head on, grazing and transmissive characteristics of SFCs for acoustic liners.

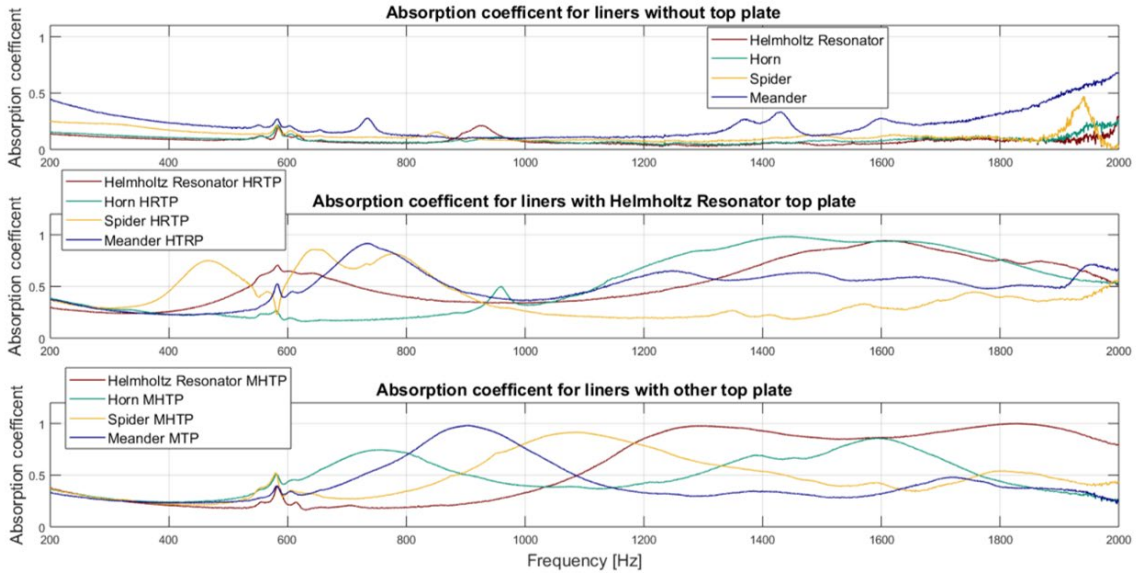

Figure 4-4 Absorption coefficient values for all tested liners

The peak frequencies are much broader than predicted and with additional multiple peaks. The baseline HR has a peak resonance of 580Hz which is within the printing tolerance resonance range 570 to 650 Hz (this also shows some of the issues with generating exact tolerances for resonators using rapid prototyping manufacturing methods). There is an additional peak at 1600Hz which is anticipated to be due to structural resonances caused by the outer edges of the test liner. As shown in Figure 2-1 smaller units are tessellated to fill the 95mm diameter or cropped Figure 2-8. The structural resonances can be reduced by framing, but design factors such as this are removed from this experimental phase to create consistency. The free walls are excited by the flow through the top plate and around the edge of the tube causing additional dominant peaks. This theory was tested in later project work when additional design factors were implemented. Furthermore, the core and top-plate are only temporally fixed rather than bonded due to limited printing resources which can lead to flow creep and coupling between units. The result of these factors is a non-ideal resonant plot, but they are more consistent with working conditions where samples are cut to fit or degrade over time, thus an understanding of the impact is valuable.

4.2.1 Mean reflection and absorption coefficients

Figure 4-5 displays the mean acoustic coefficient values for all sample configurations. For all SFCs and the HR, the introduction of a top plate increases the absorption coefficient significantly. It is also generally true that increasing the number of holes in the top plate increases the overall absorption but shifts the resonant frequency to higher values. This relationship is not linear, MTP has 2 holes compared to the 19 of HRTP which results in a 0.11 mean absorption increase, whereas HRTP to MHTP with 69 holes results in an average of 0.047 coefficient increase, this observation aligns with the perforated plate work of Bies and Handen [17].
The aim of this research is to propose an SFC acoustic liner that is comparable or better than the baseline HR. The success criteria are an increase in absorption coefficient at targeted low frequencies, at a reduced depth and weight. No SFC designs outperformed the traditional HR in absorption coefficient in these flow conditions. The best performing SFC configuration is the horn at a 3g reduction in weight. The SFC are developed in grazing flow simulation to better represent operating conditions, but the 2 microphone impedance tube was developed around the traditional HR liner thus it may not be a surprise that the HR performs best. Nonetheless the broadband attenuation offered by the SFC at a range of frequencies in the 200-2000Hz window shows the promise they have for broader low frequency noise applications. In addition, with continued research and tuning they could be well matched to the noise profile described by Khardi [6].

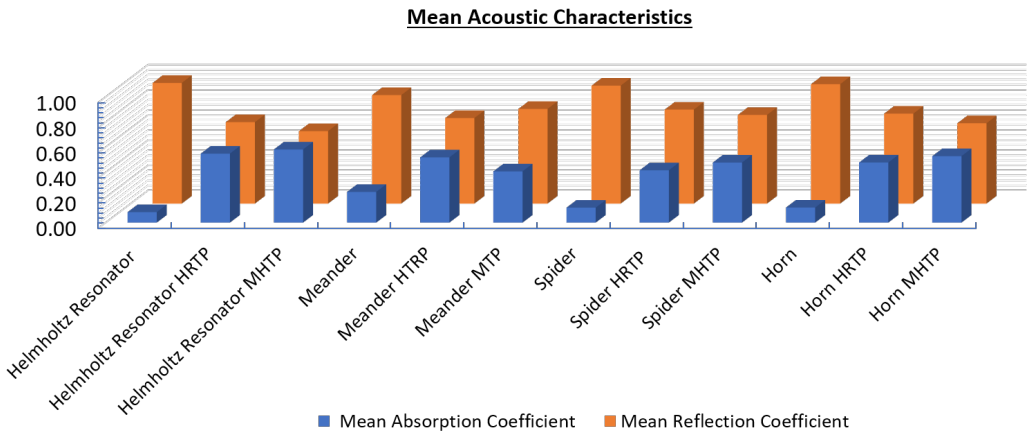

Figure 4-5 Mean reflection and absorption coefficient values

4.2.2 Resonant Peak

Figure 4-6 illustrates the comparisons of experimental and simulation (determined from origin journals) resonant peaks. The experimental data points are sized according to absorption coefficient to capture the weight for acoustic significance. The simulation data points are all set to 1, this is due to the range of data presentation in the origin papers not enabling this weighting. Generally, the peak frequencies in the paper do not align with the experimental resonant peaks indicating the grazing flow peak does not determine head on peak value.

The meander had the closest test method in the origin paper to this body of work but as seen in Figure 4-6, the peak alignment was poor, even with the Chen et al. defined MTP. The mitigations for this difference are the cropping of the design to fit the experimental tube and the lack of a framing around the core. However, with an experimental peak of triple the expected, other parameters need to be considered. There may be experimental differences and there was little detail presented by Chen et al. other than a 2-microphone impedance tube was used. Input source amplitude and flow may differ, the material characteristic instead of flow path may dominate or the bespoke rig (Figure 3-1) may be insensitive so close to the lower working frequency band. Factor such as this and more is why consistent controlled experimental comparison was needed for all liners. A simple numerical study using QWR, HR and FP theory described in section 2.2 Equation 2-2 to Equation 2-4 did show good agreement. Figure 4-6 shows the meander HRTP 11mm channel FP is 1240Hz, with QWR predicted as 621Hz. For meander HRTP 10mm channel FP is 1465Hz and QWR 730Hz. The MTP configuration does not align well with any of the classical theories. The HR is the closest, 1298Hz for the 11 mm channel, and 1123Hz for 10 mm. It could be argued that the open channel paths as seen in Figure 4-3 would allow for an extended volume reducing the resonant frequency to near 905Hz or this value lies in between the FB, QWR and HR theory as indicated in the equivalent model transfer matrix Equation 2-1, but regardless the performance was at a much higher frequency range than expected.

The spider design was defined in its origin paper as having low transmission for the full 0-2000Hz range and although transmission is not inspected here, it was predicted that this trend for the whole working frequency range would be present. Therefore, the simulation data point for the spider are set at the extremes of the range. Conversely, the spider did not show this characteristic, rather a promising multiple low frequency peak with HRTP and a monopole for the MHTP configuration. The spider did not show the broadest attenuation, or the largest mean absorption coefficient as might have been expected. Yet, if the pattern is as tuneable as indicated by Krushynska et al. it could be optimised to the characteristic noise of an aircraft, thus this low filling ratio maze-like SFC will be refined in future work.

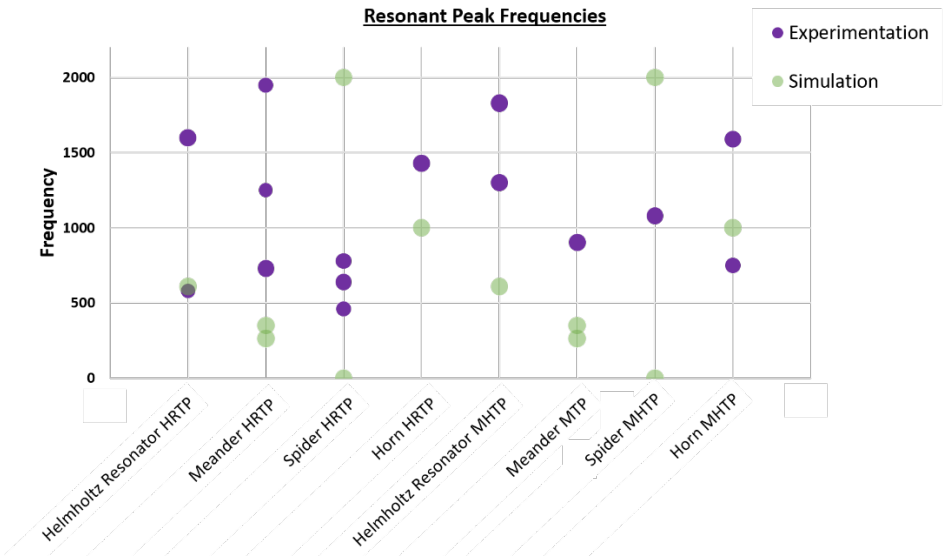

Figure 4-6 Absorption coefficient frequency peak comparison of computational and experimental data

5 CONCLUSION

The frequency agreement between the simulation data presented in the papers and this comparison was generally poor demonstrating the large variation in attenuation. Although the models could not be perfectly recreated, peaks were consistently at a higher frequency than predicted. The SFCs were chosen for their broadband and multiple resonant low frequency resonance, but this experimental work did not reliably show the multiple resonant characteristics being highly influenced by top plate configuration. This demonstrates it was essential to test liners in consistent conditions to capture a comparable acoustic performance. The origin paper deviated in experimentation and simulation methods and this standard test itself is not reflective of industrial environments. The results also indicate the difficulty of primarily reaching low frequency attenuation as many off design parameters result in higher frequency attenuation. The absorption performance of horn and spider liners showed the promise of SFCs, whether at reduced weight and comparable mean absorption to HR or multiple lower frequency absorption, respectively.

6 FUTURE WORK

The vital progression for this work is multiple environment industry-standard impedance tube tests. By using two, four microphone and grazing impedance tubes the full acoustic profile of absorption, reflection, transmission coefficients and sound transmission loss is captured in head-on, transmissive, and grazing flow. This full profile solution is a unique approach in capturing the potential of SFC design in a comparable experimental basis. The result is a ability to propose a prototype metamaterial liner adapting existing space filling curves with flow path tuned to a low frequency range specific to jet engine inlets as prescribed by work by Khardi [6].

7 REFERENCES

[1] N. Pignier, “The impact of traffic noise on economy and environment: a short literature study,” Stockholm, 2015.

[2] J. N. Glover and D. J. O’Boy, “A review of acoustic space filling curve metamaterials for jet engine inlets.,” in *Acoustics 2020, Institute of Acoustics*, 2020.

[3] B. Assouar, B. Liang, Y. Wu, Y. Li, J. C. Cheng, and Y. Jing, “Acoustic metasurfaces,” *Nat. Rev. Mater.*, vol. 3, no. 12, pp. 460–472, 2018.

[4] S. Chen *et al.*, “A review of tunable acoustic metamaterials,” *Appl. Sci.*, vol. 8, no. 9, pp. 1–

21, 2018.
[5] S. . Faruq, “An Experimental Investigation on Noise Reduction by Using Modified Helmholtz Resonator,” Bangladesh University of Engineering and Technology, 2014.
[6] S. Khardi, “An Experimental Analysis of Frequency Emission and Noise Diagnosis of Commercial Aircraft on Approach,” *Jounal Acoust. Emiss.*, vol. 26, no. 2008, pp. 290–310, 2008.
[7] Y. Wang *et al.*, “A renewable low-frequency acoustic energy harvesting noise barrier for high-speed railways using a Helmholtz resonator and a PVDF film,” *Appl. Energy*, vol. 230, pp. 52–61, 2018.
[8] D. Wu, N. Zhang, C. M. Mak, and C. Cai, “Noise Attenuation Performance of a Helmholtz Resonator Array Consist of Several Periodic Parts,” *Sensors MDPI*, vol. 5, no. 17, 2017.
[9] X. Wang, Y. Zhou, J. Sang, and W. Zhu, “A generalized model for space-coiling resonators,” *Appl. Acoust.*, vol. 158, no. 107045, 2020.
[10] J. Li and C. T. Chan, “Double-negative acoustic metamaterial,” *Phys. Rev. E - Stat. Physics, Plasmas, Fluids, Relat. Interdiscip. Top.*, vol. 70, no. 5, pp. 1–4, 2004.
[11] A. O. Krushynska, F. Bosia, M. Miniaci, and N. M. Pugno, “Spider web-structured labyrinthine acoustic metamaterials for low-frequency sound control,” *New J. Phys.*, vol. 19, no. 10, 2017.
[12] Y. Jia, Y. Luo, D. Wu, Q. Wei, and X. Liu, “Enhanced Low-Frequency Monopole and Dipole Acoustic Antennas Based on a Subwavelength Bianisotropic Structure,” *Adv. Mater. Technol.*, vol. 5, no. 4, pp. 1–6, 2020.
[13] R. Ghaffarivardavagh, J. Nikolajczyk, R. Glynn Holt, S. Anderson, and X. Zhang, “Horn-like space-coiling metamaterials toward simultaneous phase and amplitude modulation,” *Nat. Commun.*, vol. 9, no. 1, 2018.
[14] Z. Liang and J. Li, “Extreme acoustic metamaterial by coiling up space,” *Phys. Rev. Lett.*, vol. 108, no. 11, p. 114301, 2012.
[15] S. Chen *et al.*, “Engineering Coiling-Up Space Metasurfaces for Broadband Low-Frequency Acoustic Absorption,” *Phys. Status Solidi - Rapid Res. Lett.*, vol. 13, no. 12, pp. 1–6, 2019.
[16] International originisation of standards, “ISO 10534-2 Acoustics-Determination of sound absoprtion coefficent and impedance in impedance tubes- Part 2: Transfer-function methord,” Geneve, 1998.
[17] D. A. Bies and C. H. Hansen, “Muffeling Devices,” in *Engineering Noise Control: Theory and Practice*, 4th ed., CRC Press, 2009.